17th World Conference on Earthquake Engineering, 17WCEE
Sendai, Japan - September 13th to 18th 2020

3D ANALYSIS OF FRICTION PENDULUM SYSTEMS UNDER NEAR-FAULT AND LONG-PERIOD GROUND MOTIONS

N. D. Oliveto [1]

[1] *Researcher, Department of Civil and Architectural Engineering, University of Catania, Italy, noliveto@buffalo.edu*

Abstract

Considered as one of the most effective seismic protection devices, the friction pendulum (FP) system is nowadays widely used around the world. While its design and analysis are generally carried out using one-dimensional or two-dimensional models based on the principle of a linearized pendulum motion, computational models capable of describing the motion of a mass sliding with friction on a sphere may be more appropriate when assessing displacement demands under extreme events. In the present work, a three-dimensional computational formulation is developed accounting for large oscillations and the geometric nonlinearities owed to the spherical concave surfaces characterizing FP systems. The performance of these systems is then assessed under three-directional near-fault and long-period ground motions. The results are presented in the form of displacement response spectra for different values of the friction coefficient.

Keywords: seismic isolation; friction pendulum system; long-period ground motions; nonlinear modeling

1. Introduction

Seismic isolation is a widely adopted technology for the protection of building infrastructure from earthquakes. Based on the introduction of a system of low lateral stiffness devices between the building and its foundation, base isolation aims at reducing the earthquake-induced forces in the structure by shifting its fundamental period to the long-period range. Consisting of an articulated pad sliding on a spherical concave surface, one of the most effective and widely used seismic protection systems is the friction pendulum (FP) [1, 2]. As opposed to flat sliding devices, the curved sliding surface of FP systems allows to establish a recentering force. The shear force transmitted across the isolation system to the superstructure is controlled by the coefficient of friction of the sliding surfaces. Friction should be high enough to prevent sliding under low-intensity earthquakes and wind but as low as possible to limit the shear force transmitted to the structure. To achieve larger displacement capacities with no increase in the size of the devices, friction bearings with multiple sliding surfaces were conceived, namely the Double Concave Friction Pendulum (DCFP) and the Triple Friction Pendulum (TFP) bearings [3-5]. A major advantage of these systems over the single surface FP is that they allow to control the response of the system under multiple levels of ground shaking [6-8].

Friction pendulum systems have been studied extensively in the last few decades and, in their different versions, they are nowadays widely used all over the world. However, due to their relatively recent adoption for the seismic isolation of buildings and bridges, plenty critical aspects of their behavior are still under investigation. These include the dependence of the friction coefficient on contact pressure, sliding velocity and temperature [9-13], as well as the effects of vertical ground acceleration, uplift, impact and residual displacements [14-24]. For a review of current knowledge and research gaps on these topics, and some history of friction-based isolation systems, the reader is referred to [25].

After recent severe earthquakes, such as Kobe (1995) and Tohoku (2011), considerable attention has been devoted to the effects of near-fault and long-period earthquakes on the performance

of tall buildings and base-isolated structures [26-30]. However, no particular study has focused on the resonant effects of nearly periodic ground motions on friction pendulum systems. It is well known that for the low friction coefficient values used in seismic isolation, and if linear geometry is assumed, the response at resonance of a classical friction pendulum system is unbounded [31-34]. Recent analytical and numerical studies by the author [35] show that if large oscillations and non-linearities due to the spherical geometry of the system are taken into account, the displacement demands, although limited, still exceed by far the design capacities of the isolation devices. While it is common practice to analyze the behavior of FP systems using 1D [2, 36, 37] or 2D [15, 38] models based on the principle of a linearized pendulum motion, more sophisticated 3D formulations [39] should be adopted when assessing displacement demands under extreme bi-directional and tri-directional ground motions.

In the present work, a novel three-dimensional formulation is developed describing the geometrically nonlinear motion of a mass sliding with friction on a sphere. The formulation presented is used in the response simulation of FP systems under three-directional near-fault and long-period ground motions.

2. Governing equations

Shown schematically in Fig.1, FP bearings consist of an articulated pad sliding with controlled coefficient of friction, μ, on a spherical concave surface of radius R. As shown in Fig.1, we introduce a fixed cartesian coordinate system (O, X, Y, Z) defined by unit vectors $\mathbf{e}_x$, $\mathbf{e}_y$ and $\mathbf{e}_z$ along the positive X-axis, Y-axis and Z-axis, respectively. The position of the slider on the spherical surface is then identified by

$$\mathbf{r} = \mathbf{r}_h + z\mathbf{e}_z; \qquad \mathbf{r}_h = x\mathbf{e}_x + y\mathbf{e}_y \tag{1}$$

Similarly, as shown in Fig.2, the force, $\mathbf{F}$, acting on the slider is given by

$$\mathbf{F} = \mathbf{F}_h + V\mathbf{e}_z; \qquad \mathbf{F}_h = H_x\mathbf{e}_x + H_y\mathbf{e}_y \tag{2}$$

where H_x, H_y are the horizontal forces and V is the vertical force.

Fig.2 shows that if we denote by P the normal force to the sliding surface, and by $\mathbf{F}_c$ the Coulomb friction force, force $\mathbf{F}$ may be also written as

$$\mathbf{F} = \mathbf{F}_c + P\mathbf{e}_R \tag{3}$$

where $\mathbf{e}_R$ is the time varying unit vector of the normal to the sliding surface and can be written as

$$\mathbf{e}_R = \frac{\mathbf{r}_h}{R} + \left(\frac{z}{R} - 1\right)\mathbf{e}_z; \qquad z = R - \sqrt{R^2 - \mathbf{r}_h \cdot \mathbf{r}_h} \tag{4}$$

Using Eq. (2) and Eq. (4), the magnitude of the normal force, P, to the sliding surface may be computed as

$$P = \mathbf{F} \cdot \mathbf{e}_R = \mathbf{F}_h \cdot \mathbf{e}_R + V\mathbf{e}_z \cdot \mathbf{e}_R = \mathbf{F}_h \cdot \frac{\mathbf{r}_h}{R} - V\sqrt{1 - \frac{\mathbf{r}_h}{R} \cdot \frac{\mathbf{r}_h}{R}} \tag{5}$$

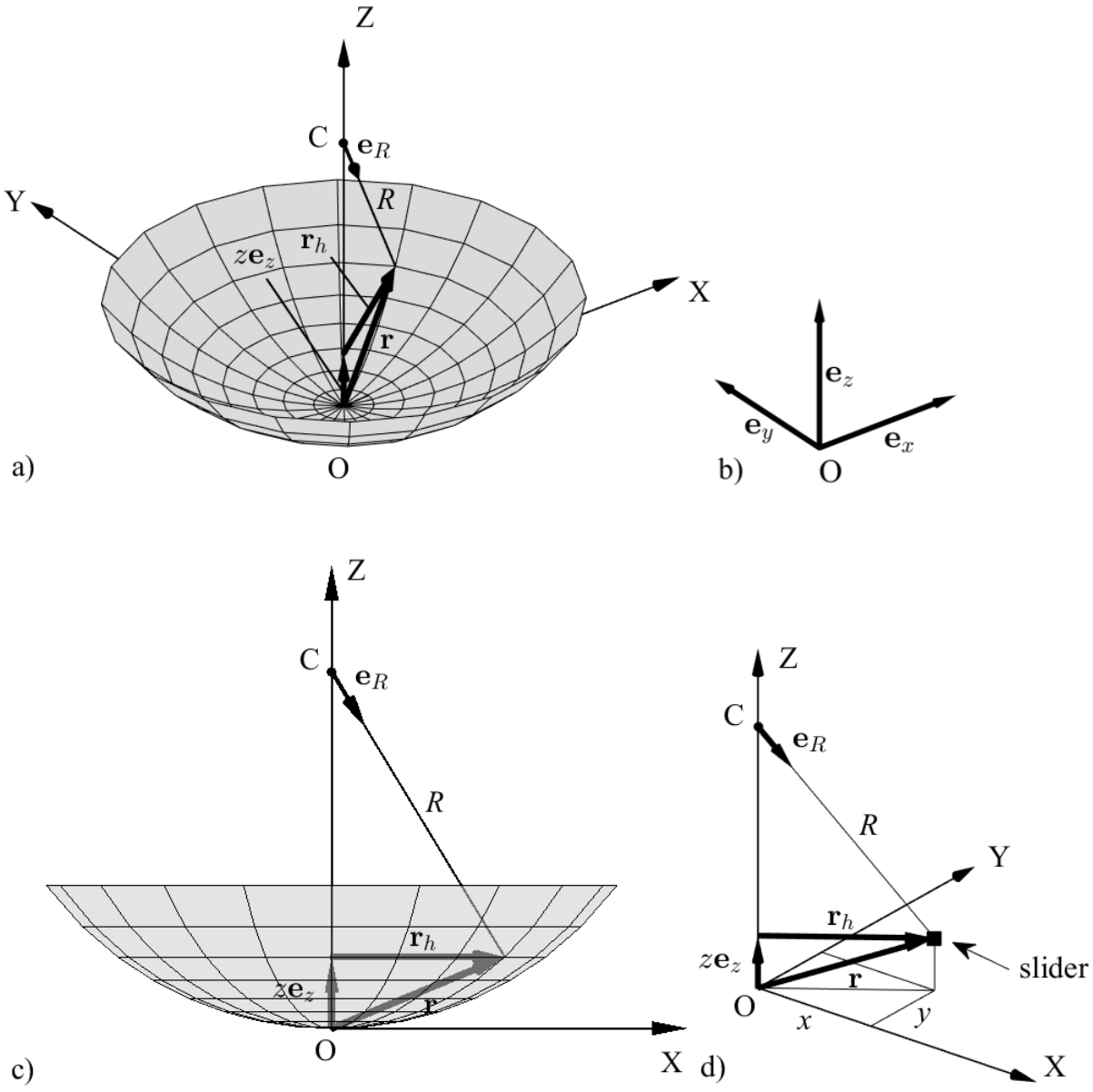

Fig. 1 – Friction Pendulum kinematics: a) 3D representation of mass sliding on spherical surface, b) unit vectors of coordinate system, c) 2D view of mass sliding on spherical surface, d) 3D representation with sliding surface omitted

The Coulomb friction force, $\mathbf{F}_c$, can be expressed as

$$\mathbf{F}_c = \mu P \frac{\dot{\mathbf{r}}}{\|\dot{\mathbf{r}}\|} \tag{6}$$

where, as shown in Fig.3,

$$\dot{\mathbf{r}} = \dot{\mathbf{r}}_h + \dot{z}\mathbf{e}_z = \dot{\mathbf{r}}_h + \frac{\mathbf{r}_h \cdot \dot{\mathbf{r}}_h}{\sqrt{R^2 - \mathbf{r}_h \cdot \mathbf{r}_h}}\mathbf{e}_z; \qquad \left\|\dot{\mathbf{r}}\right\|^2 = \dot{\mathbf{r}} \cdot \dot{\mathbf{r}} = \dot{\mathbf{r}}_h \cdot \dot{\mathbf{r}}_h + \frac{\left(\mathbf{r}_h \cdot \dot{\mathbf{r}}_h\right)^2}{R^2 - \mathbf{r}_h \cdot \mathbf{r}_h} \tag{7}$$

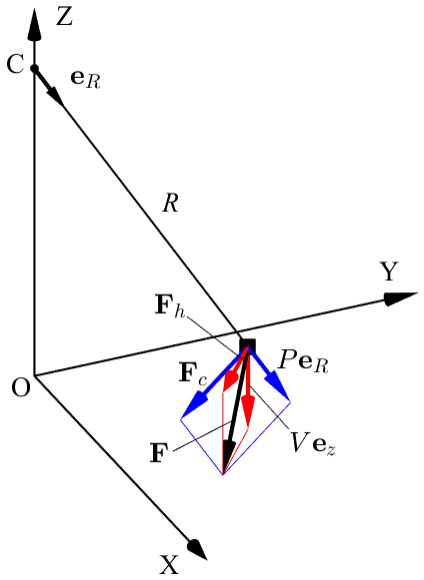

Fig. 2 – Representation of force, **F**, acting on friction pendulum slider

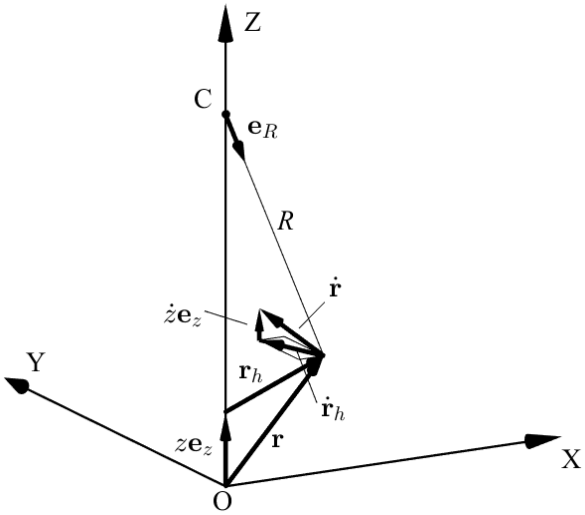

Fig. 3 – Representation of velocity vector $\dot{\mathbf{r}}$

The horizontal force $\mathbf{F}_h$ may be written as

$$\mathbf{F}_h = \left(\mathbf{F} \cdot \mathbf{e}_x\right)\mathbf{e}_x + \left(\mathbf{F} \cdot \mathbf{e}_y\right)\mathbf{e}_y \tag{8}$$

Substituting Eq. (3), Eq. (4) and Eq. (6), Eq. (8) becomes

$$\mathbf{F}_h = P\left(\mu\frac{\dot{\mathbf{r}}_h}{\|\dot{\mathbf{r}}\|}+\frac{\mathbf{r}_h}{R}\right) \tag{9}$$

Now, substituting Eq. (9) into Eq. (5) leads to

$$P = -V\frac{\sqrt{1-\frac{\mathbf{r}_h}{R}\cdot\frac{\mathbf{r}_h}{R}}}{1-\mu\frac{\dot{\mathbf{r}}_h}{\|\dot{\mathbf{r}}\|}\cdot\frac{\mathbf{r}_h}{R}-\frac{\mathbf{r}_h}{R}\cdot\frac{\mathbf{r}_h}{R}} \tag{10}$$

Finally, substituting Eq. (10) into Eq. (9), the horizontal force, $\mathbf{F}_h$, becomes

$$\mathbf{F}_h = -V\frac{\sqrt{1-\frac{\mathbf{r}_h}{R}\cdot\frac{\mathbf{r}_h}{R}}}{1-\mu\frac{\dot{\mathbf{r}}_h}{\|\dot{\mathbf{r}}\|}\cdot\frac{\mathbf{r}_h}{R}-\frac{\mathbf{r}_h}{R}\cdot\frac{\mathbf{r}_h}{R}}\left(\mu\frac{\dot{\mathbf{r}}_h}{\|\dot{\mathbf{r}}\|}+\frac{\mathbf{r}_h}{R}\right) \tag{11}$$

2.1 Equations of motion

In the case of earthquake excitation, the equations of motion of the friction pendulum system are given by

$$\begin{bmatrix} m & 0 \\ 0 & m \end{bmatrix}\ddot{\mathbf{r}}_h + \mathbf{F}_h = -\begin{bmatrix} m & 0 \\ 0 & m \end{bmatrix}\begin{bmatrix} 1 & 0 \\ 0 & 1 \end{bmatrix}\ddot{\mathbf{r}}_{hg} \tag{12}$$

where m is the mass of the superstructure. More concisely, Eq. (12) may be written as

$$\ddot{\mathbf{r}}_h + \frac{\mathbf{F}_h\left(\mathbf{r}_h,\dot{\mathbf{r}}_h\right)}{m} = -\ddot{\mathbf{r}}_{hg} \tag{13}$$

where

$$\mathbf{F}_h = -V\frac{\sqrt{1-\frac{\mathbf{r}_h}{R}\cdot\frac{\mathbf{r}_h}{R}}}{1-\mu\frac{\dot{\mathbf{r}}_h}{\|\dot{\mathbf{r}}\|}\cdot\frac{\mathbf{r}_h}{R}-\frac{\mathbf{r}_h}{R}\cdot\frac{\mathbf{r}_h}{R}}\left(\mu\frac{\dot{\mathbf{r}}_h}{\|\dot{\mathbf{r}}\|}+\frac{\mathbf{r}_h}{R}\right); \qquad V = -m\left(\ddot{z}_g+\ddot{z}+g\right); \tag{14}$$

$$\ddot{z} = \frac{\dot{\mathbf{r}}_h\cdot\dot{\mathbf{r}}_h+\mathbf{r}_h\cdot\ddot{\mathbf{r}}_h}{\sqrt{R^2-\mathbf{r}_h\cdot\mathbf{r}_h}}+\frac{\left(\mathbf{r}_h\cdot\dot{\mathbf{r}}_h\right)^2}{\left(R^2-\mathbf{r}_h\cdot\mathbf{r}_h\right)^{3/2}}$$

and $\ddot{\mathbf{r}}_{hg}$ is the vector of bidirectional horizontal ground motion. Note that vertical ground acceleration, $\ddot{z}_g$, is included through V. In the numerical simulations of the following section, nonlinear Eq. (13) is discretized in time using Newmark and solved by Newton's method.

3. Earthquake simulations

In this section, Eq. (13) is solved for a number of nearly periodic, near-fault and long-period recorded ground motions. The two horizontal components and the vertical component of each ground motion are applied simultaneously. The analyses are carried out for a wide range of periods of the isolation system and the results are presented in the form of displacement response spectra for different values of the friction coefficient, μ. The norm of the horizontal displacement vector, $\mathbf{r}_h$, normalized with respect to the radius of curvature, R, is represented in the spectra.

The first ground motion to be considered in this work is the one recorded at station SCT (Secretaria de Communicaciones y Transportes) during the 1985 Mexico City earthquake. Downloaded from the IIUNAM's Strong Motion Network (RAII-UNAM) operated at the Institute of Engineering of the National Autonomous University of México, the three components of motion, two horizontal (N00E, N90E) and one vertical (V), are shown in Fig.4. The displacement response spectra for values of the friction coefficient, μ, varying between 0.03 and 0.10 are plotted in Fig.5. Despite the modest magnitudes of horizontal and vertical ground acceleration, the displacement demands are quite significant due to the nearly-harmonic character and long duration of the ground motion.

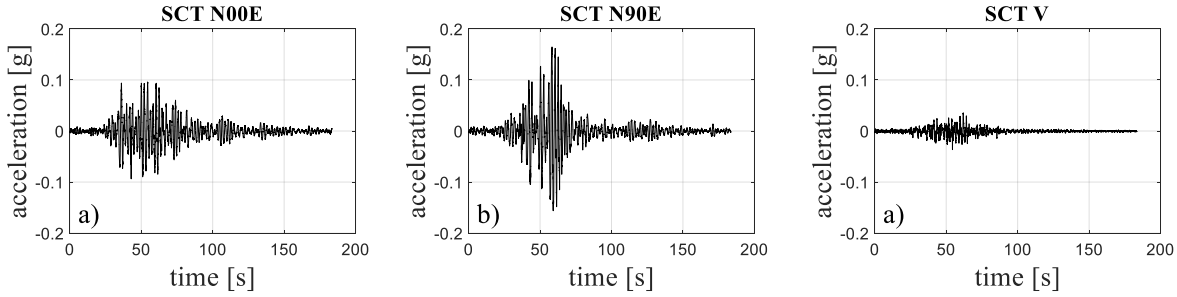

Fig. 4 – Components of ground motion recorded at station SCT during the 1985 Mexico City earthquake: a) N00E, 311 b) N90E, c) vertical

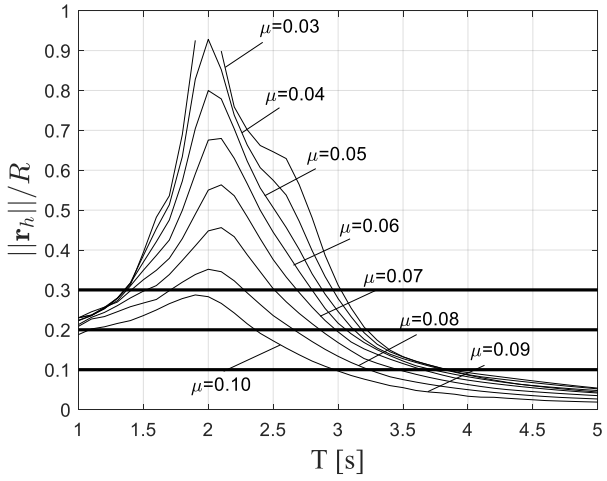

Fig. 5 – Displacement response spectra for SCT tri-directional ground motion

Three values of $\|\mathbf{r}_h\|/R$ are denoted by horizontal lines in Fig.5, namely 0.1, 0.2 and 0.3. The value of 0.1 indicates the onset of nonlinear behavior, 0.2 is a typical design limit, while 0.3 represents that value below which the error associated with the use of a geometrically linear response theory can be considered acceptable. The displacement spectra can be used to determine the combination of period, T, and coefficient of friction, μ, that the isolation system should be designed for to guarantee that the maximum allowable displacement is not exceeded.

The next ground motion to be considered was recorded in the city of Kashiwazaki, at K-NET station NIG018, during the Chuetsu-Oki 2007 earthquake. The three components of ground acceleration are shown in Fig.6. The two components of horizontal acceleration (EW and NS) are characterized by a short duration, strong low-frequency content, and a series of long-period seismic pulses typical of near-fault records [40, 41]. The displacement response spectra for values of the friction coefficient varying between 0.03 and 0.10 are plotted in Fig.7.

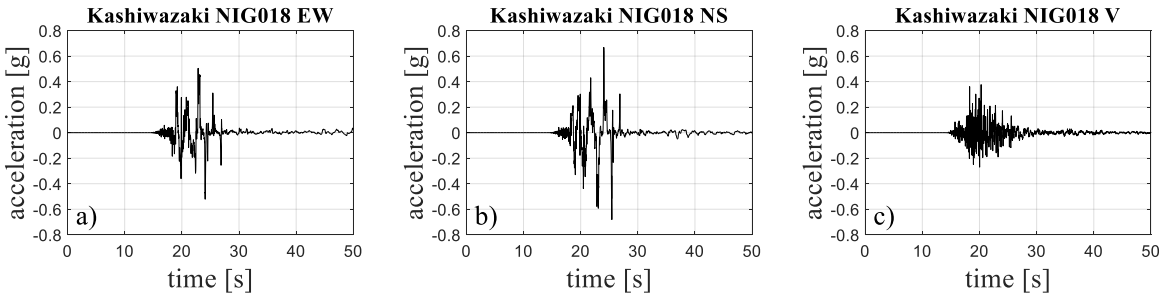

Fig. 6 – Components of ground motion recorded at K-NET station NIG018 in Kashiwazaki during the 2007 Chuetsu-Oki earthquake: a) EW, b) NS, c) vertical

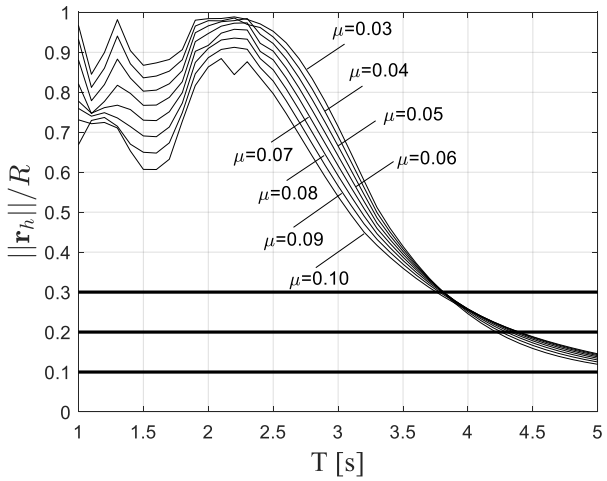

Fig. 7 – Displacement response spectra for Kashiwazaki NIG018 tri-directional ground motion

We now consider the ground motion recorded at K-NET station MYG005, in proximity of the Naruko volcano, during the 2008 Iwate–Miyagi Nairiku earthquake affecting the Tohoku region of northeastern Honshu in Japan. The three components of ground motion are shown in Fig.8 and the displacement response spectra for values of the friction coefficient varying between 0.03 and 0.1 are plotted in Fig.9.

Finally, we consider the near-fault ground motion recorded at El Centro, Southern California, during the 1979 Imperial Valley earthquake. Downloaded from the COSMOS (Consortium for

Strong-Motion Observation Systems) Strong Motion Virtual Data Center (VDC), the three components of ground motion are shown in Fig.10. In Fig.10c, we note the presence of a very strong component of vertical ground acceleration, with peaks of about 1.5 g. For a friction pendulum system with period T=3 s and coefficient of friction μ=0.03, Fig.11a shows how the strong vertical acceleration causes the normal force, *P*, to the sliding surface to switch from compression to tension, indicating uplift of the superstructure. Exactly the same happens for T=3 s and μ=0.10, as shown in Fig.11c, as well as for any other values of period, T, and coefficient of friction, μ. As shown in Fig.11b and Fig11d, no uplift occurs if vertical ground acceleration is excluded from the analysis. The displacement response spectra for values of the friction coefficient varying between 0.03 and 0.1 are plotted Fig.12. To avoid the occurrence of uplift, the vertical component of ground acceleration was not considered in this case.

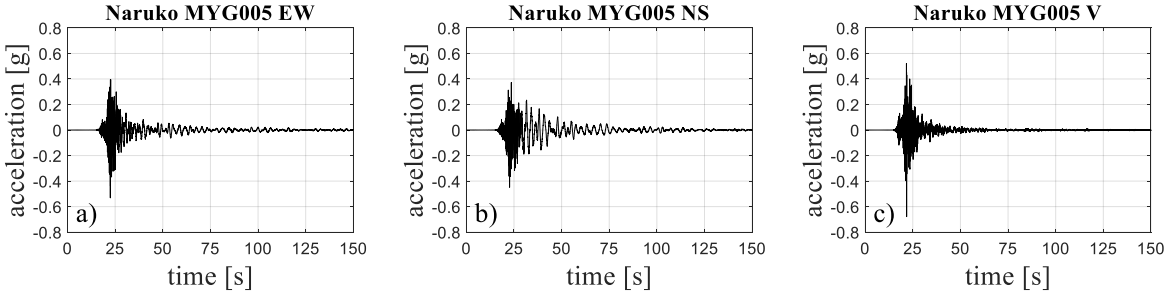

Fig. 8 – Components of ground motion recorded at K-NET station MYG005, in proximity of the Naruko volcano, during the 2008 Iwate-Miyagi Nairiku earthquake: a) EW, b) NS, c) vertical

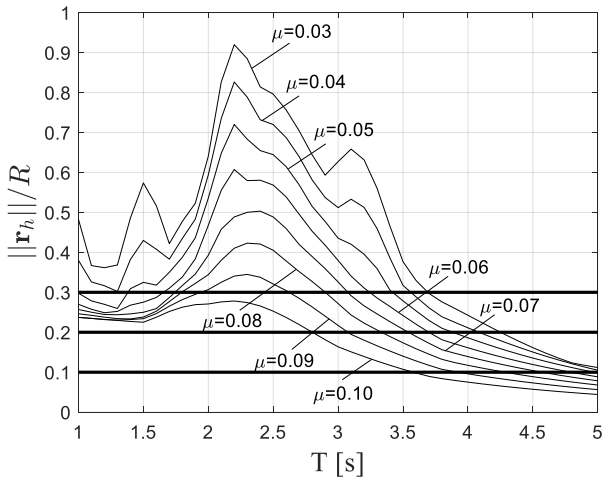

Fig. 9 – Displacement response spectra for Naruko MYG005 tri-directional ground motion

4. Conclusions

A three-dimensional formulation has been presented for the dynamic analysis of FP systems including large oscillations and the inherent nonlinearities related to the motion of a mass sliding with friction on a sphere.

Analyses carried out under a set of tri-directional near-fault and long-period recorded ground motions have shown displacement demands that exceed by far the capacity of the isolation devices in a wide range of periods. It is therefore important, when designing and implementing these systems, to

always carry out a careful seismic hazard analysis in order to exclude the occurrence of events that can cause the catastrophic failure of the isolation devices.

It has been seen that strong vertical ground accelerations can potentially determine tension forces in the friction devices and consequent uplift of the superstructure.

Extension of the current FP formulation to include effects such as the dependence of the friction coefficient on normal force, sliding velocity and temperature is the subject of ongoing work by the author.

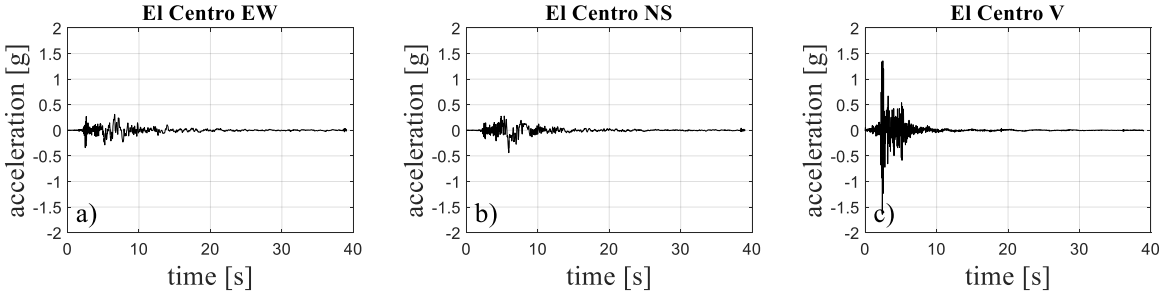

Fig. 10 – Components of ground motion recorded at El Centro during the 1979 Imperial Valley earthquake: a) EW, b) NS, c) vertical

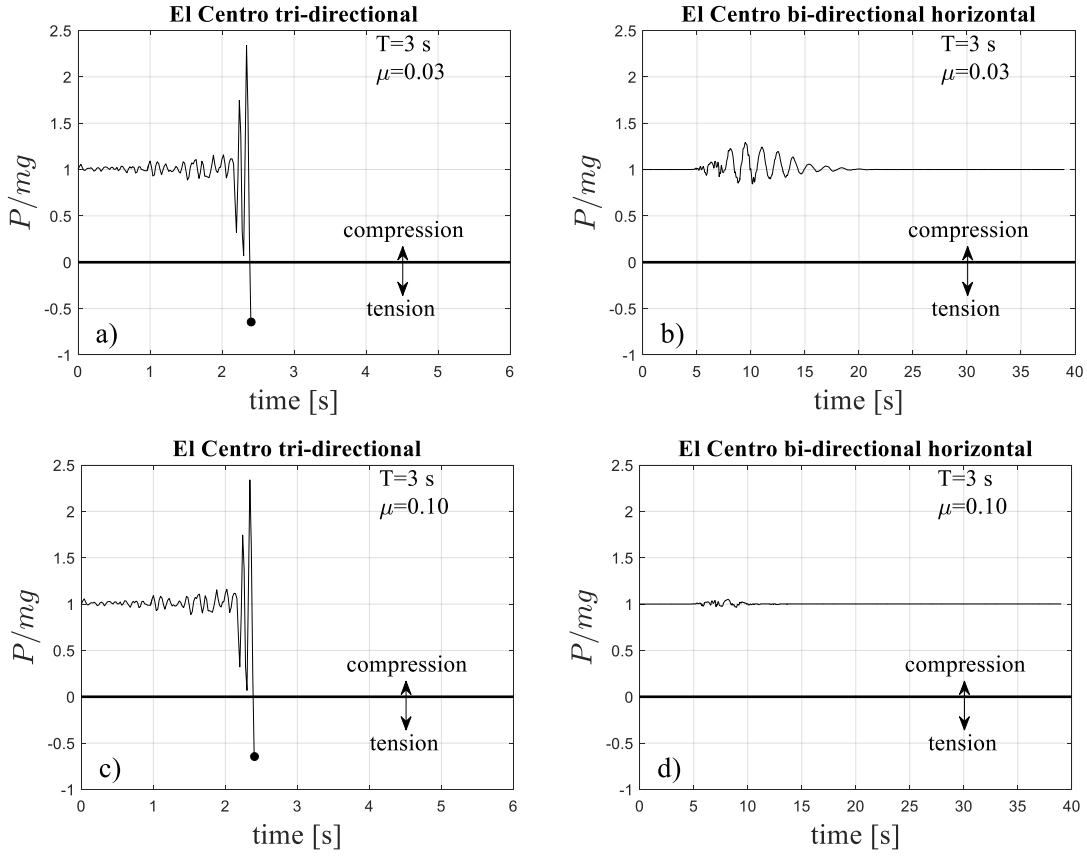

Fig. 11 – Response to El Centro earthquake in terms of normal force, *P*, to the sliding surface for FP system with period T=3 s: a) tri-directional ground motion (μ=0.03), b) bi-directional horizontal ground motion (μ=0.03), c) tri-directional ground motion (μ=0.10), d) bi-directional horizontal ground motion (μ=0.10)

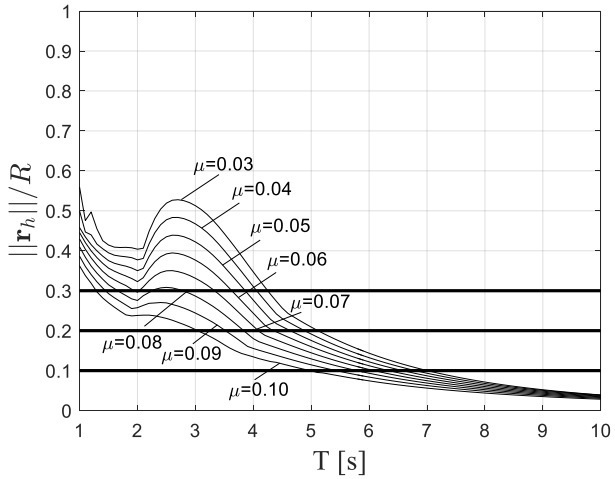

Fig. 12 – Displacement response spectra for El Centro bi-directional horizontal ground motion

5. References

[1] Zayas V, Low S, Mahin S (1987): The FPS earthquake resistant system. Experimental report UC Berkeley. (Report No. UCB/EERC-87/01).

[2] Zayas VA, Low S, Mahin S (1990): A simple pendulum technique for achieving seismic isolation. *Earthquake Spectra*, **6** (2), 317–33.

[3] Fenz DM, Constantinou MC (2006): Behavior of the double concave Friction Pendulum bearing. *Earthquake Engineering & Structural Dynamics*, **35**, 1403–24.

[4] Morgan TA (2007): The use of innovative base isolation systems to achieve complex seismic performance objectives (Ph.D. dissertation). Berkeley: Department of Civil and Environmental Engineering, University of California, USA.

[5] Fenz DM, Constantinou MC (2008): Modeling triple friction pendulum bearings for response-history analysis. *Earthquake Spectra*, **24** (4), 1011–28.

[6] Fenz DM, Constantinou MC (2008): Spherical sliding isolation bearings with adaptive behavior: theory. *Earthquake Engineering & Structural Dynamics*, **37** (2), 163–83.

[7] Fenz DM, Constantinou MC (2008): Spherical sliding isolation bearings with adaptive behavior: experimental verification. *Earthquake Engineering & Structural Dynamics*, **37** (2), 185–205.

[8] Morgan TA, Mahin SA (2010): Achieving reliable seismic performance enhancement using multi-stage friction pendulum isolators. *Earthquake Engineering & Structural Dynamics*, **39** (13), 1443–61.

[9] Constantinou MC, Whittaker AS, Kalpakidis Y, Fenz DM, Warn GP (2007): Performance of Seismic Isolation Hardware Under Service and Seismic Loading. Report No. MCEER-07-0012, Buffalo, NY, USA.

[10] Kumar M, Whittaker AS, Constantinou MC (2015): Characterizing friction in sliding isolation bearings. *Earthquake Engineering & Structural Dynamics*, **44**, 1409-1425.

[11] Furinghetti M, Pavese A, Quaglini V, Dubini P (2019): Experimental investigation of the cyclic response of double curved surface sliders subjected to radial and bidirectional sliding motions. *Soil Dynamics & Earthquake Engineering*, **117**, 190-202.

[12] De Domenico D, Ricciardi G, Benzoni G (2018): Analytical and finite element investigation on the thermo-mechanical coupled response of friction isolators under bidirectional excitation. *Soil Dynamics & Earthquake Engineering*, **106**, 131-147.

[13] De Domenico D, Ricciardi G, Infanti S, Benzoni G (2019): Frictional Heating in Double Curved Surface Sliders and Its Effects on the Hysteretic Behavior: An Experimental Study. *Frontiers in Built Environment*, **5** (74), doi: 10.3389/fbuil.2019.00074.

[14] Calvi GM, Ceresa P, Casarotti C, Bolognini D, Auricchio F (2004): Effects of axial force variation in the seismic response of bridges isolated with friction pendulum systems. *Journal of Earthquake Engineering*, **8** (1), 187-224.

[15] Mosqueda G, Whittaker AS, Fenves GL (2004): Characterization and modeling of friction pendulum bearings subjected to multiple components of excitation. *Journal of Structural Engineering (ASCE)*, **130** (3), 433-442.

[16] Ryan KL, Dao ND (2015): Influence of Vertical Ground Shaking on Horizontal Response of Seismically Isolated Buildings with Friction Bearings. *Journal of Structural Engineering (ASCE)*, **142** (1), 04015089.

[17] Sarlis AA, Constantinou MC (2013): Model of triple friction pendulum bearing for general geometric and frictional parameters and for uplift conditions. Report No. MCEER-13-0010, Buffalo, NY, USA.

[18] Sarlis AA, Constantinou MC, Reinhorn AM (2013): Shake table testing of triple friction pendulum isolators under extreme conditions. Report No. MCEER-13-0011, Buffalo, NY, USA.

[19] Masroor A, Mosqueda G (2012): Experimental simulation of base-isolated buildings pounding against moat wall and effects on superstructure response. *Earthquake Engineering & Structural Dynamics*, **41**, 2093-2109.

[20] Masroor A, Mosqueda G (2013): Impact model for simulation of base isolated buildings impacting flexible moat walls. *Earthquake Engineering & Structural Dynamics*, **42**, 357-376.

[21] Bao Y, Becker TC, Hamaguchi H (2017): Failure of double friction pendulum bearings under pulse-type motions. *Earthquake Engineering & Structural Dynamics*, **46**, 715-732.

[22] Becker TC, Bao Y, Mahin SA (2017): Extreme behavior in a triple friction pendulum isolated frame. *Earthquake Engineering & Structural Dynamics*, **46**, 2683-2698.

[23] Katsaras CP, Panagiotakos TB, Kolias B (2008): Restoring capability of bilinear hysteretic seismic isolation systems. *Earthquake Engineering & Structural Dynamics*, **37**, 557-575.

[24] Ponzo FC, Di Cesare A, Leccese G, Nigro D (2017): Shake table testing on restoring capability of double concave friction pendulum seismic isolation systems. *Earthquake Engineering & Structural Dynamics*, **46**, 2337-2353.

[25] Calvi PM, Calvi GM (2018): Historical development of friction-based seismic isolation systems. *Soil Dynamics & Earthquake Engineering*, **106**, 14-30.

[26] Ariga T, Kanno Y, Takewaki I (2006): Resonant behaviour of base-isolated high-rise buildings under long-period ground motions. *The Structural Design of Tall and Special Buildings*, **15**, 325-338.

[27] Takewaki I, Murakami S, Fujita K, Yoshitomi S, Tsuji M (2011): The 2011 off the Pacific coast of Tohoku earthquake and response of high-rise buildings under long-period ground motions. *Soil Dynamics & Earthquake Engineering*, **31**, 1511-1528.

[28] Takewaki I, Fujita K, Yoshitomi S (2013): Uncertainties in long-period ground motion and its impact on building structural design: Case study of the 2011 Tohoku (Japan) earthquake. *Engineering Structures*, **49**, 119-134.

[29] Sato E, Furukawa S, Kakehi, A, Nakashima M (2011): Full-scale shaking table test for examination of safety and functionality of base-isolated medical facilities. *Earthquake Engineering & Structural Dynamics*, **40**, 1435-1453.

[30] Shi Y, Kurata M, Nakashima M (2014): Disorder and damage of base-isolated medical facilities when subjected to near-fault and long-period ground motions. *Earthquake Engineering & Structural Dynamics*, **43**, 1683-1701.

[31] Den Hartog JP. LXXIII (1930): Forced vibrations with combined viscous and coulomb damping. *The London, Edinburgh, and Dublin Philosophical Magazine and Journal of Science*, **9** (59), 801-817.

[32] Den Hartog JP, Mikina SJ (1932): Forced vibrations with nonlinear springs. *Transactions of the American Society of Mechanical Engineers (ASME)*, **54**, 157-164.

[33] Den Hartog JP (1984): *Mechanical vibrations*. New York: Dover Publications, Inc.

[34] Chopra AK (2012): *Dynamics of Structures*. Prentice Hall: New Jersey.

[35] Oliveto ND (2020): Nonlinear dynamic analysis of friction pendulum systems under harmonic, near-fault and long-period ground motions. *Journal of Engineering Mechanics (ASCE)*, under review.

[36] Mokha A, Constantinou MC, Reinhorn AM, Zayas VA (1991): Experimental Study of Friction-Pendulum Isolation System. *Journal of Structural Engineering*, **117** (4), 1201-1217.

[37] Barone S, Calvi GM, Pavese A (2017): Experimental dynamic response of spherical friction-based isolation devices. *Journal of Earthquake Engineering*, DOI: 10.1080/13632469.2017.1387201.

[38] Ryan KL, Chopra AK (2004): Estimating the seismic displacement of friction pendulum isolators based on non-linear response history analysis. *Earthquake Engineering & Structural Dynamics*, **33**, 359-373.

[39] Monti G, Petrone F (2016): Analytical thermo-mechanics 3D model of friction pendulum bearings. *Earthquake Engineering & Structural Dynamics*, **45**, 957-977.

[40] Somerville PG (2002): Characterizing Near Fault Ground Motion for the Design and Evaluation of Bridges. *Third National Seismic Conference and Workshop on Bridges and Highways*, Portland, Oregon, USA.

[41] Somerville PG (2005): Engineering characterization of near fault ground motions. *2005 NZSEE Conference: Planning and Engineering for Performance in Earthquakes*, Wairakei Resort, Taupo, New Zealand.

